Available online at www.sciencedirect.com
SCIENCE DIRECT®
Comput. Methods Appl. Mech. Engrg. 195 (2006) 4371–4382
Computer methods in applied mechanics and engineering
www.elsevier.com/locate/cma

On the use of pseudo-forces to consider initial conditions in 3D time- and frequency-domain acoustic analysis

C.J. Martins [a], J.A.M. Carrer [b], W.J. Mansur [c,*], F.C. Araújo [d]

[a] Department of Civil Production Engineering, CEFET, 30510-000 Belo Horizonte, MG, Brazil
[b] PPGMNE/Federal University of Paraná, CP 19011, 81531-990 Curitiba, PR, Brazil
[c] Department of Civil Engineering, COPPE/UFRJ, CP 68506, CEP 21945-970 Rio de Janeiro, RJ, Brazil
[d] Department of Civil Engineering, UFOP, 35400-000 Ouro Preto, MG, Brazil

Received 17 February 2004; received in revised form 13 September 2005; accepted 14 September 2005

Abstract

This work is mainly concerned with a general strategy, based on well known concepts of classical mechanics, for taking into account initial conditions in frequency-domain (FD) and time-domain (TD) analyses. A general approach, extended here to three-dimensional applications, is presented. Special problems associated with analyses through Discrete-Fourier-Transform (DFT) algorithms, as those occurring in consequence of a non-correct choice of extended period or those connected with aliasing phenomenon, are also discussed. Furthermore, an alternative starting procedure for time-marching schemes (in TD analyses) is proposed. At the end of the paper, to validate the proposed techniques and to demonstrate their generality, two- and three-dimensional problems with non-homogeneous initial conditions are solved through frequency- and time-domain approaches by employing the Finite Element Method (FEM). Numerical results are compared with existing analytical solutions.

Keywords: Finite element method; 3D wave equation; Frequency- and time-domain analyses; Initial conditions

1. Introduction

According to the nature of the dynamic problem to be solved, the numerical solution can be sought either in the time-domain or in transformed domains. Although time-domain formulations can be efficiently adopted for solving a great range of problems, in some cases the analysis via transformed domains (e.g. frequency, Laplace or wavelet domains) is the only feasible alternative [25,7,11]. Particular attention will be devoted here to the frequency-domain approach [25,7,22] that has been extensively used in analyses in which the physical parameters, such as the damping in soil–structure interaction problems, are frequency-dependent. Practical problems in which the analyses of dynamic systems are carried out in the frequency domain are presented by Wolf [28], related to soil–structure interaction problems, Clough and Penzien [7], related to structural systems, Hall [12] and Kinsler [15], related to FEM modeling of acoustic problems, and Beskos [3], Dominguez [8], Brebbia [4] and Banerjee [1], related to engineering problems modeled with the BEM.

A great deal of attention has been devoted to turn the frequency-domain approach more efficient. One of the deficiencies of the Fourier analysis, as described by Thomson [25], Clough and Penzien [7], Paz [22], Oppenheim and Schafer [21], is

* Corresponding author.
E-mail address: webe@coc.ufrj.br (W.J. Mansur).

0045-7825/$ - see front matter © 2005 Elsevier B.V. All rights reserved.
doi:10.1016/j.cma.2005.09.007

concerned with the periodic nature of the Fourier transform and, consequently, with the difficulty of considering initial conditions. In spite of the importance of this topic, to the best of the authors' knowledge, only a few works concerning this matter have been presented until now. Venancio-Filho and Claret [27] presented the concept of the Implicit Fourier Transform (ImFT), extended later to non-linear problems by Mansur et al. [17]. Veletsos and Ventura [26] employed the Green's function and its time derivative in modal coordinate analyses, and in Soares and Mansur [24] the inverse discrete Fourier transform of the steady state Green's function is carried out to obtain the corresponding time-domain Green's function for SDOF mechanical systems. The techniques described above, in spite of being efficient and of taking into account initial conditions, are applied to problems described by modal coordinates (i.e., SDOF mechanical systems).

The present work describes a quite general method to take into account initial conditions. The proposed method, which is based on the concepts of pseudo-forces, see Refs. [9,18], and generalized functions [6], will be applied to the solution of three- and two-dimensional scalar problems, in the time- and frequency-domain, modeled with finite elements. Initially, the time-dependent and frequency-dependent partial differential equations governing wave propagation problems are presented. Then the corresponding algebraic systems of equations are shown. A discussion concerning DFT-based analysis, which emphasizes the special role played by the extended period of analysis and by the aliasing phenomenon in the acquisition of the numerical response, is also presented.

The steps adopted to take into account the initial conditions, related to the potential and its time derivative, in frequency-domain analyses are presented. In addition, the method previously presented by Mansur et al. [18] for 2D problems is extended to 3D frequency- and time-domain applications.

Finally, aiming at validating the described algorithms, the results from the analyses of two- and three-dimensional problems with non-homogeneous initial conditions, in time- and frequency-domain, are presented and compared with analytical results.

2. The wave propagation problem

The scalar wave equation is usually associated with the description of vibrational phenomena, such as the vibration of strings and membranes, and the propagation of acoustic waves and electric signals along wires. In its general form, the associated initial boundary value problem is given by (see [19,20])

$$\rho \frac{\partial^2 u(\mathbf{x},t)}{\partial t^2} - \nabla \cdot (E \nabla u(\mathbf{x},t)) = f(\mathbf{x},t) \quad \text{in } \Omega, \tag{1}$$

with the boundary conditions

$$\begin{aligned} u(\mathbf{x},t) &= \overline{u}(\mathbf{x},t) \quad \text{on } \Gamma_u, \\ p(\mathbf{x},t) &= \frac{\partial u(\mathbf{x},t)}{\partial \mathbf{n}(\mathbf{x})} = \overline{p}(\mathbf{x},t) \quad \text{on } \Gamma_p \end{aligned} \tag{2}$$

and the initial conditions

$$u(\mathbf{x},0) = u_0(\mathbf{x}) \quad \text{in } \Omega, \tag{3}$$

$$\dot{u}(\mathbf{x},0) = \dot{u}_0(\mathbf{x}) \quad \text{in } \Omega. \tag{4}$$

In the above equations $u(\mathbf{x}, t)$ denotes the scalar solution, $f(\mathbf{x}, t)$ the domain source function, and ρ and E the medium density and Young's modulus respectively.

The solution of Eq. (1), under harmonic excitations, can be assumed to behave harmonically with angular frequency ω, if a long enough time has elapsed after the occurrence of initial disturbances. In this way, the problem is said to be stationary. The physical variables of the acoustic problem can be represented as follows:

$$u(\mathbf{x},t) = U(\mathbf{x},\omega)e^{i\omega t}, \quad f(\mathbf{x},t) = F(\mathbf{x},\omega)e^{i\omega t}, \quad p(\mathbf{x},\mathrm{t}) = P(\mathbf{x},\omega)e^{i\omega t}, \tag{5}$$

where $U(\mathbf{x}, \omega)$, $F(\mathbf{x}, \omega)$ and $P(\mathbf{x}, \omega)$ are complex functions. After substituting expressions (5) into Eq. (1) and eliminating the exponential function $e^{i\omega t}$, the resulting Helmholtz's equation can be written as

$$\rho\omega^2 U(\mathbf{x},\omega) + \nabla \cdot (E \nabla U(\mathbf{x},\omega)) = -F(\mathbf{x},\omega) \quad \text{in } \Omega. \tag{6}$$

The boundary conditions to Eq. (6) are given by

$$\begin{aligned} U(\mathbf{x},\omega) &= \overline{U}(\mathbf{x},\omega) \quad \text{on } \Gamma_u, \\ P(\mathbf{x},\omega) &= \overline{P}(\mathbf{x},\omega) \quad \text{on } \Gamma_p. \end{aligned} \tag{7}$$

2.1. Spatial discretization

The Finite Element Method (FEM) was adopted as a numerical tool for the solution of the scalar wave Eq. (1) (see [29,2,14]). The resulting system of linear algebraic equations can be written as

$$\mathbf{M}\ddot{\mathbf{U}} + \mathbf{C}\dot{\mathbf{U}} + \mathbf{K}\mathbf{U} = \mathbf{R}. \tag{8}$$

Matrices **M**, **C** and **K** represent, respectively, mass, damping and stiffness global matrices.

For harmonic problems, one has $\mathbf{U}(t) = \mathbf{U}^{\omega}e^{i\omega t}$ and $\mathbf{R}(t) = \mathbf{R}^{\omega}e^{i\omega t}$ ($\mathbf{U}^{\omega}$ and $\mathbf{R}^{\omega}$ represent the nodal potential and nodal flux amplitudes respectively); thus the corresponding system of equations reads

$$(-\omega^2\mathbf{M} + i\omega\mathbf{C} + \mathbf{K})\mathbf{U}^{\omega} = \mathbf{R}^{\omega}. \tag{9}$$

2.2. Damping

A usual way to add damping to the system is by expressing its viscous damping matrix, **C**, proportional to the mass and stiffness matrices (Rayleigh's damping model). By assuming stiffness-proportional damping, say $c = a_1 E$ (c denotes the viscous damping coefficient associated with the continuum model), its implementation in the FD formulations can be directly carried out by substituting Young's modulus, E, by the following complex one:

$$E^d = E(1 + i\omega a_1), \quad \text{with } a_1 = \frac{c}{E}; \text{ hence } E^d = E + i\omega c. \tag{10}$$

As seen above, the viscous damping assumes frequency-dependent energy dissipation. This assumption is sometimes non-realistic (see [25,7]). Indeed, experimental observations show that the dissipated energy is frequency-independent for a great deal of materials employed in engineering at a wide frequency range. In this case, the following frequency-independent damping model (hysteretic damping) should be used instead

$$E^d = E(1 + ig), \tag{11}$$

where g is the hysteretic damping coefficient.

2.3. Nyquist frequency

In order to obtain the solution of transient dynamic problems by a frequency-domain formulation, the Fourier transform is applied to the time-dependent excitation. Subsequently, after the response spectrum is determined (i.e. solving Eq. (9)), the synthesis of the frequency-dependent spectrum is carried out via inversion. The number of time sampling points must be chosen so that the highest excitation frequency in the Fourier spectrum be higher than the highest frequency (that matters) of the discretized mechanical system at hand (see [21,23,5]); this excitation frequency is the so-called Nyquist frequency, defined as

$$\omega_{\mathrm{Nyq}} = \frac{N\pi}{T}, \tag{12}$$

where N is the number of sampling points and T is the total time of analysis. The consequence of the violation of this condition is an incorrect superposition of effects, leading to a distortion of the inverse Fourier transform (aliasing phenomenon).

2.4. Extended period

The Fourier transform is based on the assumption that the external excitation and the system response are periodic in time. Hence, to attain a correct response to a non-periodic loading, it is necessary to extend the time of analysis up to a time T_p, *the extended period*, so that at T_p the system is at rest. If T_p is large enough, the causality condition is obeyed, i.e., perturbations acting before the initial time will not influence the response in the interval of interest. Since the prediction of the extended period, T_p, is inadvisable in practice, it must be estimated. In previous works, e.g. Refs. [17,24], the extended period has been estimated as a time interval longer than any time required to damp down the first mode contribution (measured, for instance, in terms of displacement amplitudes) to h percent of its initial contribution. Thus, by following this approach, the extended period can be established according to the relation

$$T_p \geqslant \frac{\ln(100/h)}{\xi_1\omega_1}, \tag{13}$$

where ξ_1 is the damping ratio associated with the first mode and ω_1 is the fundamental frequency of the system. Usually, 1% is adopted for h.

3. Contribution of initial conditions to transient problems

The correct specification of the initial conditions plays an important role in the description of time-dependent problems. The method developed here introduces initial conditions via pseudo-forces in 3D frequency- and time-domain modeling. The time-domain strategy is new, and so is the 3D frequency-domain approach, which allows for non-trivial initial conditions [25,7,22].

3.1. Initial displacement

First, only the initial displacement field is imposed to the system. The initial velocity field is assumed to be null and no external forces are applied. The basic step consists in substituting the initial displacement field by static pseudo-forces which generate the given initial displacement field. An equivalent pseudo-force vector, $\mathbf{F}_\mathbf{U}$, is obtained according to $\mathbf{F}_\mathbf{U} = \mathbf{K}^{-1}\mathbf{U}_0$, $\mathbf{U}_0$ being the known nodal initial displacement vector. Note that $\mathbf{F}_\mathbf{U}$ is an external static force vector, applied to the system previously to the initial time of the analysis, which generates the initial field $\mathbf{U}_0$. The system motion starts by the application of a nodal equivalent force vector $-\mathbf{F}_\mathbf{U}$ at $t = 0$, which generates a displacement field $\Delta\mathbf{U}^\mathrm{t}$, computed by

$$\mathbf{M}\Delta\ddot{\mathbf{U}}^\mathrm{t} + \mathbf{C}\Delta\dot{\mathbf{U}}^\mathrm{t} + \mathbf{K}\Delta\mathbf{U}^\mathrm{t} = -\mathbf{F}_\mathbf{U}H(t) = -\mathbf{K}\mathbf{U}_0H(t), \tag{14}$$

where $H(t)$ is the Heaviside function (or unit-step function), see [20]. One can assume that the total displacement field, $\mathbf{U}^\mathrm{t}$, for the present case, is constituted of two parts: one due to the action of the field force represented by $\mathbf{F}_\mathbf{U}H(t)$ and the other due to the initial displacement field. Thus

$$\mathbf{U}^\mathrm{t} = \Delta\mathbf{U}^\mathrm{t} + \mathbf{U}_0. \tag{15}$$

In frequency-domain analyses, the equivalent pseudo-force vector, $\mathbf{F}_\mathbf{U}$, is incorporated to the system by following a similar procedure. The final equation is

$$(-\omega^2\mathbf{M} + \mathrm{i}\omega\mathbf{C} + \mathbf{K})\Delta\mathbf{U}^\omega = -\mathbf{F}_\mathbf{U}H^\omega = -\mathbf{K}\mathbf{U}_0H^\omega, \tag{16}$$

where ω is the Fourier transform parameter and H^ω is the Fourier transform of the Heaviside function. Analogously to expression (15), the total complex displacement field can be computed as a sum of two parts, as follows:

$$\mathbf{U}^\omega = \Delta\mathbf{U}^\omega + \delta(\omega)\mathbf{U}_0. \tag{17}$$

It is important to note that if the DFT (or FFT) algorithm is employed, the Heaviside function, $H(t)$, must be replaced by the product $H(t)[1 - H(t - T/2)]$. In this case, the extended period must be considered twice that of the initial guess (obtained for instance from expression (13)).

3.2. Initial velocity

The contribution due to an initial velocity field can be obtained from the following concepts of classical mechanics (under the assumption of constant mass, [10,16]):

Momentum (**Q**): The momentum is a conservative quantity. It is defined as follows:

$$\mathbf{Q} = m\mathbf{v}. \tag{18}$$

Impulse (**I**): The impulse is defined as the time integral of the force, given by

$$\mathbf{I} = \int_0^{\Delta t} \mathbf{F}\,\mathrm{d}t = m\int_0^{\Delta t} \frac{\mathrm{d}\mathbf{v}}{\mathrm{d}t}\,\mathrm{d}t. \tag{19}$$

The impulse–momentum relation states that the impulse **I** acting on the mass will result in a change in the momentum and, consequently, in its velocity. If the mass is initially at rest, one can write

$$\mathbf{I} = m\mathbf{v}_0. \tag{20}$$

Then, the contribution of an initial velocity field, $\mathbf{V}_0 = \dot{\mathbf{U}}(0)$, can be taken into account by the pseudo-force $\mathbf{F}_\mathbf{V}$ defined below [20,6]

$$\mathbf{F}_\mathbf{V} = \mathbf{M}\dot{\mathbf{U}}(t)\delta(t), \tag{21}$$

where $\delta(t)$ is the Dirac delta function. Thus, the displacement $\mathbf{U}^{\mathrm{t}}$ due to the presence of an initial velocity field can be computed from

$$\mathbf{M}\ddot{\mathbf{U}}^{\mathrm{t}} + \mathbf{C}\dot{\mathbf{U}}^{\mathrm{t}} + \mathbf{K}\mathbf{U}^{\mathrm{t}} = \mathbf{F}_{\mathbf{V}} = \mathbf{M}\dot{\mathbf{U}}(t)\delta(t). \tag{22}$$

In the frequency domain, the Fourier transform of the Dirac delta function is equal to the unity, hence the corresponding transformed equation of motion is given by

$$(-\omega^2\mathbf{M} + \mathrm{i}\omega\mathbf{C} + \mathbf{K})\mathbf{U}^{\omega} = \mathbf{M}\mathbf{V}_0. \tag{23}$$

It must be observed that the Fourier transform of $\mathbf{F}_{\mathbf{V}}$, which is equal to $\mathbf{M}\mathbf{V}_0$, must be corrected when DFT algorithms are employed. As shown by Clough and Penzien [7]: $\mathrm{DFT}(\mathbf{M}\mathbf{V}_0\delta(t)) = \frac{1}{N\Delta t}\mathbf{M}\mathbf{V}_0$, where $N\Delta t = T$.

3.3. General case

When the structure is subjected to the action of external forces $\mathbf{R}^{\mathrm{t}}$ under non-homogeneous initial conditions $\mathbf{U}_0$ and $\mathbf{V}_0$, the system of equations is written as (in the time-domain)

$$\mathbf{M}\Delta\ddot{\mathbf{U}}^{\mathrm{t}} + \mathbf{C}\Delta\dot{\mathbf{U}}^{\mathrm{t}} + \mathbf{K}\Delta\mathbf{U}^{\mathrm{t}} = \mathbf{R}^{\mathrm{t}} - \mathbf{K}\mathbf{U}_0 H(t) + \mathbf{M}\dot{\mathbf{U}}(t)\delta(t), \tag{24}$$

where

$$\mathbf{U}^{\mathrm{t}} = \Delta\mathbf{U}^{\mathrm{t}} + \mathbf{U}_0. \tag{25}$$

Alternatively to classical starting procedures for time-marching schemes (see [2,14]), the time-step procedure can be initialized using the new initial conditions in the deformed state, given by

$$\Delta\mathbf{U}^0 = \Delta\dot{\mathbf{U}}^0 = \mathbf{0}. \tag{26}$$

In this case, the loading vector of the dynamic equilibrium equation, Eq. (24), is given by

$$\mathbf{R}^{\mathrm{t}} - \mathbf{K}\mathbf{U}_0 + \frac{\mathbf{M}\mathbf{V}_0}{\Delta t} \quad \text{at } t = 0 \quad \text{and} \quad \mathbf{R}^{\mathrm{t}} - \mathbf{K}\mathbf{U}_0 \quad \text{for } t > 0. \tag{27}$$

In frequency-domain analyses, the complex response in the transformed domain is obtained from

$$(-\omega^2\mathbf{M} + \mathrm{i}\omega\mathbf{C} + \mathbf{K})\Delta\mathbf{U}^{\omega} = \mathbf{R}^{\omega} - \mathbf{K}\mathbf{U}_0 H^{\omega} + \mathbf{M}\mathbf{V}_0, \tag{28}$$

where the complex displacement field is given by

$$\mathbf{U}^{\omega} = \Delta\mathbf{U}^{\omega} + \delta(\omega)\mathbf{U}_0. \tag{29}$$

4. Applications

4.1. Rod under a Heaviside type forcing function and initial conditions prescribed all over the domain

In this example, a prismatic rod fixed at one end and free at the other is analyzed (see [31]). For the discretization, 4000 lagrangean linear hexahedral elements where employed, which gives 4961 degrees of freedom, see Fig. 1. The rod length is $L = 1.2$ m and its cross-section area is $A = 0.3\ \mathrm{m} \times 0.3\ \mathrm{m}$. The longitudinal wave propagation velocity and density are respectively $c = 1000$ m/s and $\rho = 0.01\ \mathrm{kg/m^3}$. The rod is subjected to the initial conditions

$$\begin{cases} U_0 = \dfrac{p_0 L}{E}\cdot\dfrac{z}{L}, & 0 \leqslant z \leqslant L, \\ V_0 = \dfrac{p_0 c}{E}, \quad c = \sqrt{\dfrac{E}{\rho}} & 0 \leqslant z \leqslant L, \end{cases} \qquad \text{with } p_0 = 100\ \mathrm{N/m^2}. \tag{30}$$

In expressions (30), E is the Young's modulus. Additionally, a Heaviside type-forcing function $p_0 H(t)$ is applied at the free end of the rod. This problem was analyzed through the time- and frequency-domain formulations. For the FD analysis, the extended period $T_p = 0.196$ s and 4096 sampling points were adopted. It must be pointed out that the extended period, T_p, calculated by considering modal damping ratio $\xi_1 = 0.0125$ and modal frequency $\omega_1 \cong 1309$ rad/s, corresponds to $h = 4\%$ (i.e., reduction to 4% of the first mode contribution). In the TD analysis, the implicit damped HHT scheme [13] was used with: $\Delta t = 0.00005$ s, $\alpha = -\frac{1}{9}, \gamma = \frac{1}{2} - \alpha, \beta = \frac{(1-\alpha)^2}{4}$, and total time of analysis $T_a = 0.0096$ s (192 time steps). In the FD analysis, a hysteretic damping coefficient $g = 2\xi_1 = 0.025$ was adopted. The proportionality factor used for taking into account a similar viscous damping (adjusted by the first mode) proportional to the stiffness matrix [7] is then $a_1 = 1.91 \times 10^{-5}$. Figs.

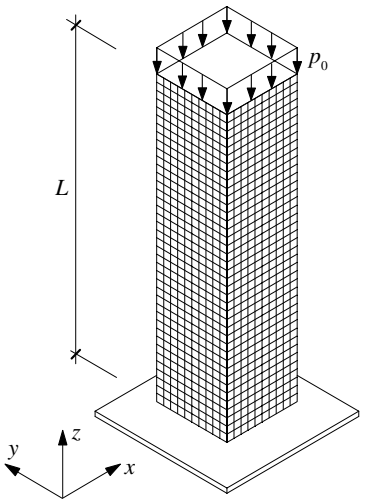

Fig. 1. Rod discretization: 4961 nodes, 4000 linear hexahedral elements.

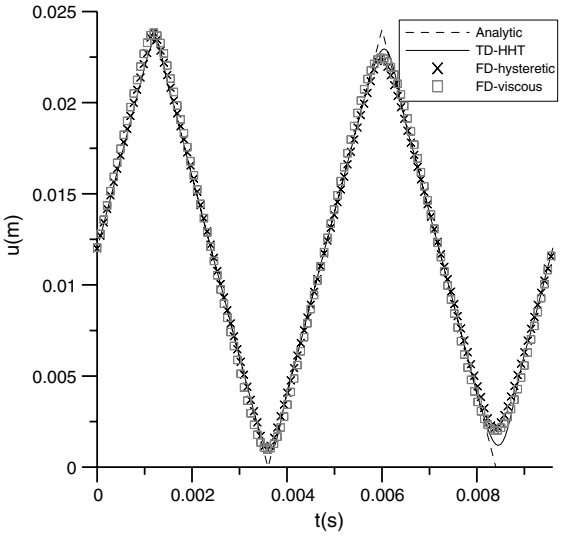

Fig. 2. Displacement time-history at the free end of the rod under Heaviside-type forcing function and initial conditions prescribed all over the domain.

2 and 3 present the response at the free end of the rod in terms of displacement and velocity, respectively. A good agreement between numerical and analytical responses is observed.

4.2. Rod under a Heaviside type forcing function and initial conditions prescribed in part of the domain

In this example, the following initial conditions are imposed to the rod analyzed in the previous example:

$$\begin{cases} U_0 = \dfrac{1}{4}\dfrac{p_0 L}{E}\cdot\left(z-\dfrac{3L}{4}\right)\dfrac{4}{L}, \quad \dfrac{3L}{4}\leqslant z\leqslant L, \\ V_0 = \dfrac{p_0 c}{E}, \quad c=\sqrt{\dfrac{E}{\rho}}, \quad \dfrac{3L}{4}\leqslant z\leqslant L, \qquad \text{with } p_0 = 100\ \text{N/m}^2. \\ V_0 = U_0 = 0, \quad 0\leqslant z<\dfrac{3L}{4}, \end{cases} \tag{31}$$

Again, the HHT time-marching scheme was adopted for the time-domain analysis with the same parameters α, β, and γ, the same time step and total time of analysis as in the previous example. The values of the hysteretic and viscous damping coefficients are the same as well. Once more, the results agree quite well with each other. Figs. 4 and 5 present, respectively, the displacement and velocity at the free end of the rod.

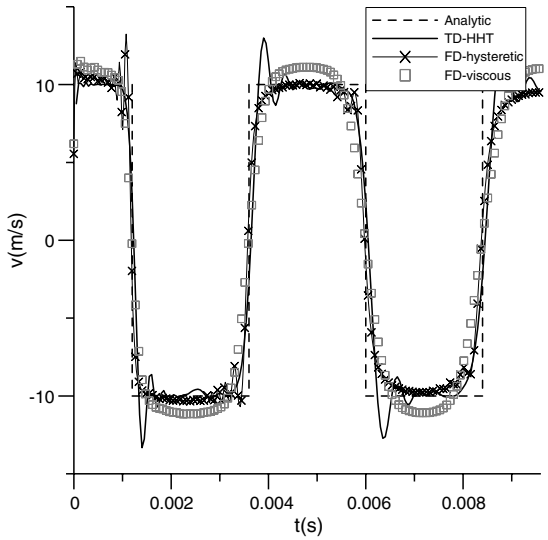

Fig. 3. Velocity time-history at the free end of the rod under Heaviside-type forcing function and initial conditions prescribed all over the domain.

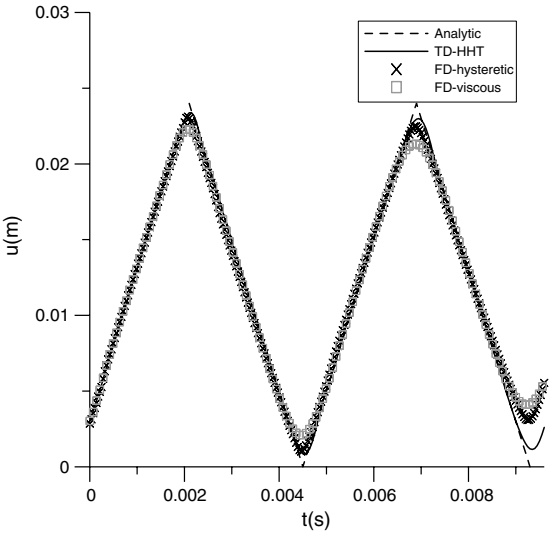

Fig. 4. Displacement time-history at the free end of the rod under Heaviside-type forcing function and initial conditions prescribed in part of the domain.

4.3. Square membrane under prescribed initial velocity: 3D and 2D analyses

This example consists of a square membrane of side $L = 50$ cm, subjected to zero initial displacements in its entire domain and the initial velocity field described below (see Fig. 6):

$$V_0 = \begin{cases} \dfrac{100c}{EA}, & \text{if } \left[\dfrac{L}{4} \leqslant x \leqslant \dfrac{3L}{4}\right] \cap \left[\dfrac{L}{4} \leqslant y \leqslant \dfrac{3L}{4}\right] \cap [0 \leqslant z \leqslant h], \\ 0, & \text{in the remainder of the domain.} \end{cases} \tag{32}$$

The following parameters were adopted: $c = 1000$ cm/s and $\rho = 0.01$ kg/cm^3. In the 2D analysis, 20,000 isoparametric linear triangular elements were adopted. In the 3D analysis 2500 isoparametric parabolic continuum elements were employed (see Fig. 7). In the frequency-domain analyses, 4096 sampling points and an extended period $T_p = 2.5$ s, estimated to reduce the contribution of the first mode ($\omega_1 \cong 89$ rad/s, $\xi_1 = 0.05$) to $h = 1.49 \times 10^{-3}\%$ of its initial contribution, were adopted. In the TD analysis, the implicit HHT method was applied to march on time. $\Delta t = 0.0001$ s and 1250 time-steps were employed. A hysteretic damping coefficient $g = 2\xi_1 = 0.10$ was adopted. The corresponding stiffness-proportional viscous-damping factor (adjusted by the first mode, and used for both HHT and viscous-damping frequency-domain analyses) is $a_1 = 1.13 \times 10^{-3}$. Note that a TD analysis without damping via HHT scheme with parameters $\alpha = 0.00$, $\beta = 0.25$, and $\gamma = 0.50$ was also carried out.

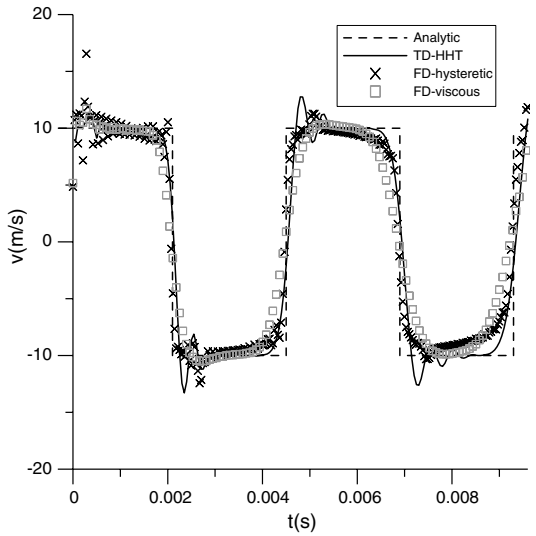

Fig. 5. Velocity time-history at the free end of the rod under Heaviside-type forcing function and initial conditions prescribed in part of the domain.

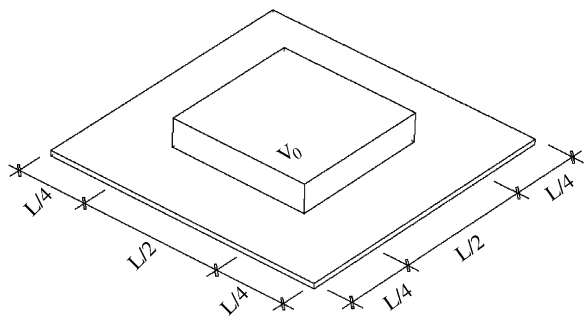

Fig. 6. Square membrane under prescribed initial velocity field.

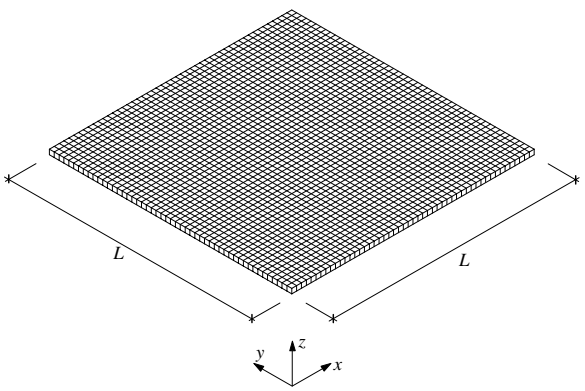

Fig. 7. 3D spatial discretization of the square membrane: 30,603 nodes, 2500 quadratic prismatic elements.

Figs. 8 and 9 show, respectively, the results related to the vertical displacement and velocity at point A$(25, 25, 0)$ at the centre of the membrane. In Figs. 10 and 11, results at point B$(12.5, 12.5, 0)$ obtained from the 3D analysis is compared with the corresponding analytical solution (see [19,31]). A good agreement is observed between analytical and numerical responses. The results obtained from the 2D analysis are not shown, since they are very close to the 3D ones.

With the purpose of observing the influence of the extended period on the response determined through FD analyses, the membrane shown in Fig. 6 is analyzed again with different extended periods. Namely, the following pairs of T_p values and sampling points were considered: $T_p = 2.5$ s and $N = 2048$; $T_p = 1.25$ s and $N = 1024$; $T_p = 0.625$ s and $N = 512$; $T_p = 0.3125$ s and $N = 256$; and $T_p = 0.1563$ s and $N = 128$. These values of the extended period correspond, respectively,

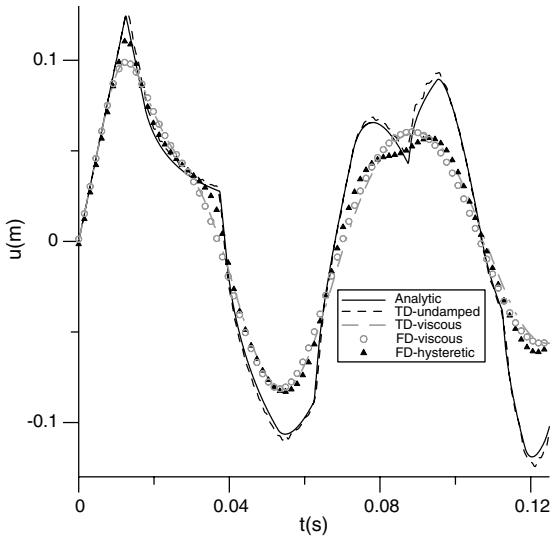

Fig. 8. Displacement time-history at the center of the square membrane.

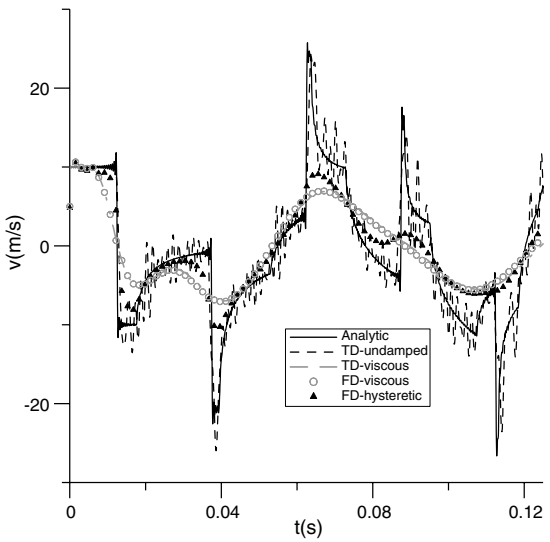

Fig. 9. Velocity time-history at the center of the square membrane.

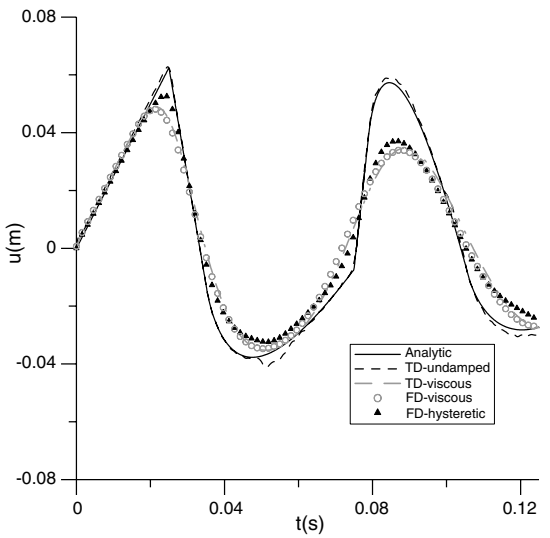

Fig. 10. Displacement time-history at the point B(12.5, 12.5, 0) for the square membrane.

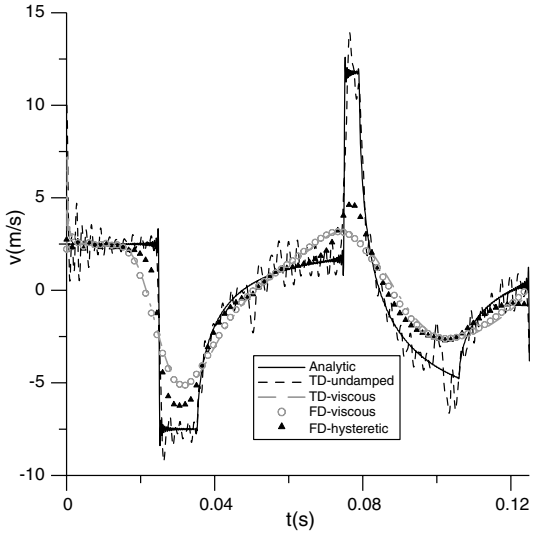

Fig. 11. Velocity time-history at the point B(12.5, 12.5, 0) for the square membrane.

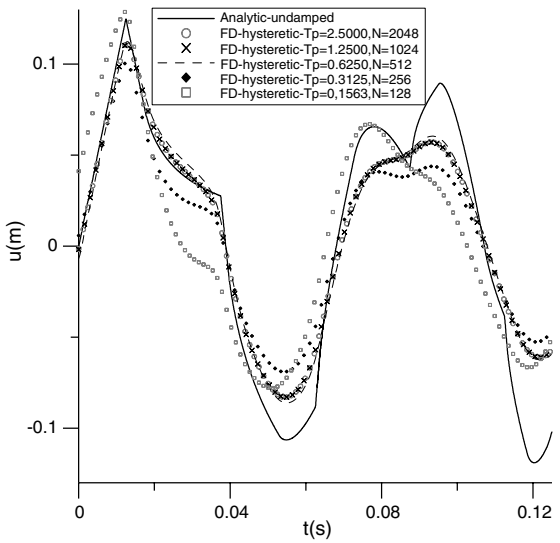

Fig. 12. Displacement time-history at the central point of the square membrane for different extended periods T_p.

to h values of approximately 1.49×10^{-3}%, 0.39%, 6.22%, 24.9% and 49.9%, respectively. The time reconstitution of the displacement at the centre of the membrane is presented in Fig. 12.

In Fig. 13, the velocity time-history at the centre of the membrane, obtained by employing the Central Difference [29] and the Fourth Order Finite Difference [30] explicit algorithms (TD analyses), is presented. The classic initialization procedure as well the initialization procedure proposed here, were adopted. As in the case of the previous TD analyses, 1250 time steps of length $\Delta t = 0.1$ ms and no damping were considered.

5. Conclusions

This work is concerned with the presentation and validation of a unified approach that enables one to compute the contribution of initial conditions in time- and frequency-domain analyses. Basically, the approach consists in expressing the initial conditions in terms of suitable pseudo-forces. As shown here, the method is quite general, i.e., frequency-domain equations are directly obtained from corresponding time-domain ones. The examples presented confirm its applicability and generality, encouraging its further extension to elastodynamics. In all cases analyzed, a quite good agreement with the analytical solutions was attained (see Figs. 2–5, 8–11). As observed in Fig. 12, the correct choice of the extended period T_p plays an important role in a reliable representation of the causality. A very short value of T_p brings perturbations at the

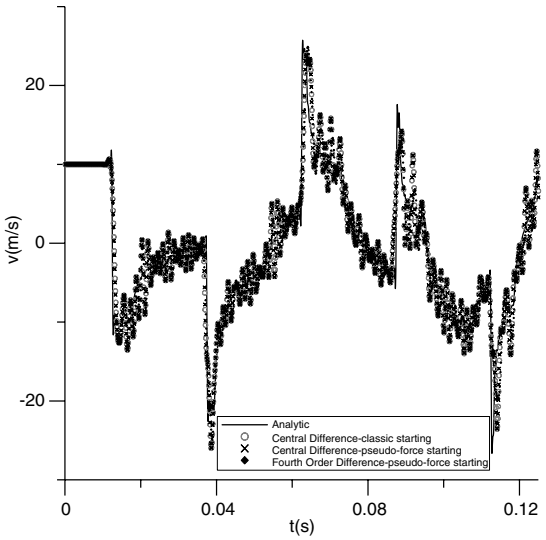

Fig. 13. Pseudo-force starting procedure versus standard starting procedure in time domain.

initial time due to previous time history, i.e. the causality condition is not verified; otherwise, if T_p is too long the analysis cost will be increased.

On the other hand, the responses shown in Fig. 13, obtained through TD analyses also indicate that the proposed initialization procedure can be adopted in the most general case of initial conditions. It is important to notice that the use of this initialization procedure can be very attractive from the computational point of view, since the inversion of the mass matrix in implicit time-marching schemes becomes unnecessary.

The Finite Element Method (FEM) was used here. Nevertheless, the pseudo-force method is independent of the numerical approach adopted and can be applied with other numerical methods, for instance, the Finite Difference Method (FDM) or the Boundary Element Method (BEM).

References

[1] P.K. Banerjee, The Boundary Element Method in Engineering, McGraw-Hill, New York, 1994.
[2] K.J. Bathe, Finite Element Procedures, Prentice-Hall Inc., Englewood Cliffs, NJ, 1996.
[3] D.E. Beskos, G.D. Manolis, Boundary Element Methods in Elastodynamics, Springer-Verlag, 1987.
[4] C.A. Brebbia, J.C.F. Telles, L.C. Wrobel, Boundary Element Techniques, Springer-Verlag, 1984.
[5] E.O. Brigham, The Fast Fourier Transform, Prentice-Hall Inc., Englewood Cliffs, NJ, 1974.
[6] A. Butkov, Mathematical Physics, Addison-Wesley, 1968.
[7] R.W. Clough, J. Penzien, Dynamics of Structures, McGraw-Hill, Berkeley, 1993.
[8] J. Dominguez, Boundary Elements in Dynamics, Computational Mechanics Publications & Elsevier, London, 1993.
[9] W.G. Ferreira, A.M. Claret, F. Venancio-Filho, W.J. Mansur, F.S. Barbosa, A frequency-domain pseudo-force method for dynamic structural analysis: nonlinear systems and non-proportional damping, J. Brazil. Soc. Mech. Sci. XXII (4) (2000) 551–564.
[10] A.P. French, Mecánica Newtoniana, Editora Reverté, Barcelona, 1974.
[11] H. Grundmann, E. Trommer, Transform methods-what can they contribute to (computational) dynamics? Comput. Struct. 79 (2001) 2091–2102.
[12] D. Hall, Basic Acoustics, Krieger Publishing Company, 1987.
[13] H.M. Hilber, T.J.R. Hughes, R.L. Taylor, Improved numerical dissipation for time integration algorithms in structural dynamics, Earthquake Engrg. Struct. Dynam. 5 (3) (1977) 283–292.
[14] T.J.R. Hughes, The Finite Element Method: Linear Static and Dynamic Finite Element Analysis, second ed., Prentice-Hall, New Jersey, 2000.
[15] L.E. Kinsler, A.R. Frey, A.B. Coppens, J.V. Sanders, Fundamentals of Acoustics, third ed., John Wiley & Sons, New York, 1982.
[16] L.E. Malvern, Introduction to the Mechanics of a Continuous Medium, Prentice-Hall Inc., Englewood Cliffs, NJ, 1969.
[17] W.J. Mansur, W.G. Ferreira, F. Venancio-Filho, A.M. Claret, J.A.M. Carrer, Time segmented frequency-domain analysis for non-linear multi-degree-of-freedom structural systems, J. Sound Vib. 237 (2000) 457–475.
[18] W.J. Mansur, D.J. Soares, M.A.C. Ferro, Initial conditions in frequency-domain analysis: the FEM applied to the scalar wave equation, J. Sound Vib. 270 (4–5) (2004) 767–780.
[19] P.M. Morse, K.U. Ingard, Theoretical Acoustics, McGraw-Hill, New York, 1968.
[20] P.M. Morse, H. Feshbach, Methods of Theoretical Physics, McGraw-Hill, New York, 1953.
[21] A.V. Oppenheim, R.W. Schafer, Discrete Time Signal Processing, second ed., Prentice-Hall Inc., Englewood Cliffs, NJ, 1989.
[22] M. Paz, Structural Dynamics—Theory and Computation, fourth ed., Chapman and Hall, New York, 1997.
[23] J.G. Proakis, D.G. Manolakis, Digital Signal Processing—Principles, Algorithms and Applications, third ed., Prentice-Hall Inc., Englewood Cliffs, NJ, 1996.
[24] D.J. Soares, W.J. Mansur, An efficient time/frequency domain algorithm for modal analysis of non-linear models discretized by the FEM, Comput. Methods Appl. Mech. Engrg. 192 (2003) 3731–3745.

[25] W.T. Thomson, Theory of Vibration with Applications, first ed., Prentice-Hall Inc., Englewood Cliffs, NJ, 1973.
[26] A. Veletsos, C. Ventura, Efficient analysis of dynamic response of linear systems, Earthquake Engrg. Struct. Dynam. 12 (1984) 521–536.
[27] F. Venancio-Filho, A.M. Claret, Matrix formulation of the dynamic analysis of SDOF systems in the frequency domain, Comput. Struct. 42 (5) (1992) 853–855.
[28] J.P. Wolf, Dynamic Soil–Structure Interaction, Prentice-Hall Inc., Englewood Cliffs, NJ, 1985.
[29] O.C. Zienkiewicz, R.L. TaylorThe Finite Element Method, vols. 1 and 2, McGraw-Hill, 1989.
[30] J.A.M. Carrer, C.J. Martins, L.A. Sousa, A fourth order finite difference method applied to elastodynamics: finite element and boundary element formulations, Struct. Engrg. Mech. 17 (6) (2004) 735–749.
[31] W.J. Mansur, A time-stepping technique to solve wave propagation problems using the boundary element method, Ph.D. Thesis, Southampton University, 1983.